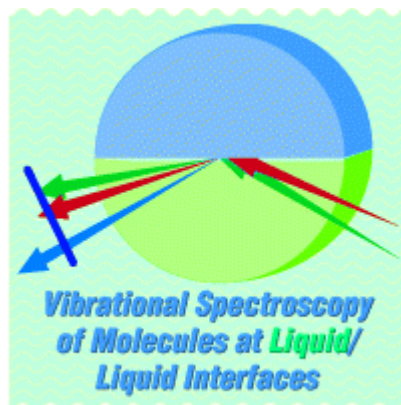


Analytical Chemistry News & Features  
September 1, 1997; pp. 536 A-543 A.  
Copyright © 1997 American Chemical Society  
S0003-2700(97)09020-3

[AC Home](#)[Contents](#)[Search](#)

# Vibrational Spectroscopy of Molecules at Liquid/Liquid Interfaces

## id Interfaces

*Because liquid surfaces and interfaces play a central role in everyday life, understanding their structure and dynamics on the molecular level is important.*

G. L. **Richmond**  
*University of Oregon*

Liquid surfaces and interfaces play a central role in many of the chemical and physical processes in our lives. Exchange of molecules and ions across liquid or membrane surfaces is prevalent in biological processes. Many environmentally important chemical separation processes are based on the partitioning of solute molecules across the interface between two immiscible liquids. Respiration in the lungs of living organisms occurs across lipid surfactant monolayers. The ordering of organic molecules at liquid interfaces to form supramolecular structures upon transfer to a solid is being used in molecular recognition, catalysis, and nonlinear optical applications.

Understanding such processes requires a knowledge of the structure and dynamics of these liquid interfaces on a molecular level. Our knowledge of the properties of these interfaces has come primarily from theoretical studies and experimental measurements of a more macroscopic nature. Development of several experimental techniques has recently advanced our knowledge about molecular structure at liquid-air interfaces. Neutron (1) and X-ray (2) diffraction and reflection studies have provided structural details on an angstrom level about molecular packing at the liquid-air interface. From optical techniques such as Fourier transform-IR (3), Brewster angle microscopy (4), fluorescence microscopy (5), sum frequency vibrational spectroscopy (SFVS) (6-8), and second harmonic generation (SHG) (8-11), information about the phase behavior and structure and orientation of molecules at this interface has been obtained. (Glossary of abbreviations found on page 539 A.)

Progress has been much slower in understanding the molecular structure at the interface between two bulk liquids because of inapplicability or lack of surface specificity of most surface techniques for probing this interface. Studies using fluorescent probes (12) that adsorb at this interface have been particularly useful, as have resonant and nonresonant SHG studies (10, 11, 13, 14).

In the past few years, my co-workers and I have developed a way to measure the vibrational spectra of molecules adsorbed at the interface between two immiscible liquids using a technique called total internal reflection sum frequency vibrational spectroscopy (TIR-SFVS) (15, 16). The combination of the unique selectivity of SFVS in measuring the molecular spectra of surface molecules and the enhanced sensitivity provided by the TIR geometry makes TIR-SFVS a powerful technique for measuring molecular structure at this interface. This Report provides an overview of the technique, examples of the type of information that can be obtained, and some thoughts about opportunities for future applications.

## **Principles**

SFVS is a nonlinear optical method used to measure the vibrational spectra of surface molecules with inherent

discrimination against molecules in the adjacent bulk liquid. Pioneered by Shen (8), it is based on the second-order optical phenomenon called sum frequency generation (SFG), which consists of illuminating the surface of a solid or liquid with two overlapping pulsed laser beams of different frequencies,  $\omega_1$  and  $\omega_2$ . At the surface, the intense optical fields induce a second-order polarization of the medium at  $\omega_1 \pm \omega_2$ .

This higher order polarization results in the production of a coherent optical field, which for SFG is at the summed frequency. The surface sensitivity of SFG arises from the asymmetry of an interface relative to the adjacent bulk liquid, gas, or solid. Under the electric dipole approximation, second-order nonlinear optical processes are forbidden from occurring in bulk centrosymmetric media. Consequently, the characteristics of the SF response reflect the molecular properties of the interface.

Typically for SFVS, one of the laser beams is fixed at a visible frequency, and the second is tunable within the IR region

of the spectrum of interest (Figure 1 top). Because of the relatively weak nature of this second-order polarization, pulsed lasers are generally used, and the higher peak powers of shorter pulses are preferred. The SF light produced at the interface occurs in both reflectance and transmittance at an angle a few degrees removed from the linear reflection and transmission angles.

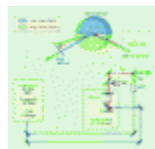


**Figure 1. Diagram of the experimental setup and cell design.**

(a) The IR ( $\omega_{IR}$ ) and the visible ( $\omega_{VIS}$ ) 532-nm beams are incident through the high-index  $CCl_4$  phase. (b) Nd:YAG laser and the optical parametric oscillator (OPO) used to generate the IR pulses. (Adapted from ref. 15.)

Obtaining a vibrational spectrum of a molecule with SFG

relies on an optical resonance between the tunable IR beam  $\omega_{\text{IR}}$  and the frequency of the vibrational transition in the molecule  $\omega_{\text{v}}$ . As  $\omega_{\text{IR}}$  is tuned over a molecular resonance in the surface molecule of interest, the efficiency of the SFG process is correspondingly enhanced. There is always an additional nonresonant background contribution, which is usually quite small for liquid surfaces and interfaces. The strength of the resonant SFG response depends on several factors--the surface density of the molecule of interest, the linewidth of the transition, the IR transition moment, and the Raman transition strength. The last two factors restrict the technique to the study of vibrational modes that are both IR and Raman active. Beyond the surface sensitivity, an additional advantage is that the detected SFV signal occurs in the visible region, where detectors are relatively efficient. Disadvantages include low signal levels and difficulties in determining a quantitative relationship between the peak intensities and the number of molecules being sampled.

SFVS has been used to study various liquid surface processes (11) such as monolayers at the air-water interface (6, 17, 18), the SFV spectrum of water at the air-water (19) and oil-water (20) interfaces, alcohols at the liquid-vapor interface (21), and the surface of aqueous solutions of acetonitrile (22). Many studies have examined molecular adsorbates at solid surfaces in ultrahigh vacuum (23), electrochemical (24), and ambient (25) environments.

### Glossary of abbreviations

SFG	Sum frequency generation
SHG	Second harmonic generation
TIR	Total internal reflection
SFG	Sum frequency generation
OPO	Optical parametric oscillator
KTP	Potassium titanium phosphate
OPA	Optical parametric amplifier
SDS	Sodium dodecyl sulfate

SDS	Sodium dodecyl sulfate
DAC	Dodecylammonium chloride
PC	Phosphatidylcholine
DLPC	Dilauroyl-PC
DMPC	Dimyristoyl-PC
DPPC	Dipalmitoyl-PC
DSPC	Distearoyl-PC

## **Instrumentation and experimental considerations**

In TIR-SFVS studies of liquid-liquid interfaces, the incident beams are sent through the higher index medium at the critical angle for each particular beam as shown in Figure 1 top (15). For our experiments, in which CCl<sub>4</sub> and H<sub>2</sub>O or D<sub>2</sub>O are used as the bulk liquids, the IR and visible beams are brought through the CCl<sub>4</sub> solution at the appropriate angles as determined by expressions given elsewhere (26). The SFVS response is collected in reflection at the corresponding critical angle for the sum frequency. We find that the enhancement in the SF response using the TIR geometry is 4-5 orders of magnitude higher than what we obtain using an external reflection geometry. This enhancement has allowed us to work with relatively low-incident photon densities, minimizing the risk of thermal heating. We found a similar enhancement in the TIR SHG response, which has been useful in studies of alkane-water interfaces (14) and the interface between two immiscible electrolyte solutions (13).

One of the current limitations of the technique is the lack of availability of nanosecond or picosecond IR laser sources that are broadly tunable over the IR region. Most studies have been restricted to regions of the IR where tunable laboratory laser sources are available. We have found two laser systems that are quite successful in the 2- to 4- $\mu$ m region. The simplest system consists of a LiNbO<sub>3</sub> optical parametric oscillator (OPO), which is pumped with the fundamental output of a Q-switched Nd:YAG laser

generating 1064-nm pulses at 10 Hz with a pulse duration of 12 ns (Figure 1 bottom). Tunability throughout the desired wavelength region

is achieved by angle tuning the LiNbO<sub>3</sub> crystal. IR light pulses in the 2700-3100 cm<sup>-1</sup> region with a bandwidth of 6 cm<sup>-1</sup> and energies of 2-3 mJ are obtainable over this spectral region. The visible probe beam is the remainder of the 1064-nm YAG fundamental output, which is frequency doubled to generate 532 nm. The advantages of this system lie in its relatively low cost and low maintenance. The disadvantage is in the limited wavelength region accessibility. Other Nd:YAG-pumped IR laser systems that have been used in this region vary in the pulse duration of the pump laser and nonlinear crystals used (6, 11, 18, 24).

An alternative system that offers promise for extended wavelength tunability consists of a Ti:sapphire regenerative amplifier laser system, which is used to pump potassium titanium phosphate (KTP) crystals in a two-stage optical parametric amplifier (OPA) seeded with a small portion of white-light continuum (27). This system currently produces IR pulses tunable from 2.4 to 4.0 μm at a repetition rate of 1 kHz. The energy of the pulses over this range is ~10 μJ with a bandwidth of 18 cm<sup>-1</sup> and a pulse duration of 1.9 ps. The IR pulses are combined at the interface with the 800-nm light from the Ti:sapphire regenerative amplifier. With appropriate optics, the bandwidth of this laser can readily be narrowed. More importantly, with the use of other nonlinear crystals to generate IR light, it should be possible to probe vibrational transitions in the range of 1-8 μm.

The studies conducted thus far in our laboratory have focused on molecules studied at a CCl<sub>4</sub>-H<sub>2</sub>O or CCl<sub>4</sub>-D<sub>2</sub>O interface. This is the simplest oil-water system to study from a spectroscopic viewpoint because of the transparency of the CCl<sub>4</sub> to the IR wavelengths accessible with our laser systems. The spectroscopic measurements are complemented by surface tension measurements made by the Wilhelmy plate method.

### **Simple ionic surfactants**

Surfactant production has increased tremendously over the

past two decades because of the rise in applications of these compounds. Although most surfactants are still used for conventional purposes, such as washing and cleaning, they are also widely used in stabilizing foams and emulsions in beverage and food processing, in stabilizing particulate dispersions, and in the secondary recovery of oil from porous rock beds. All of these uses depend on the amphiphilic character of the molecule--part nonpolar hydrophobic hydrocarbon and part polar hydrophilic moiety. The need to satisfy the conflicting characteristics of the molecule and minimize the energy of the system leads to a host of complex structural features of these molecules in the bulk solution (e.g., micelles and vesicles) as well as at interfaces where they form monolayers of different phases.

When a surfactant adsorbs at an oil-water interface, the hydrophilic portion, or head group, remains in the aqueous phase, whereas the hydrophobic end, or tail, is solvated by the oil phase. Although much has been learned in recent years about how variations in the hydrophilic and hydrophobic portion of the molecules lead to different structural features at the air-water interface, little is known about their behavior at the more complex oil-water interface. For example, what effect does the nonpolar solvent have on the van der Waals interactions between the hydrophobic alkyl chains of the molecule as the solvent penetrates the chain structure? At an air-water interface, such attractive forces can counter the repulsion between the similarly charged head groups at the interface. What type of balance between these two effects is struck at the oil-water interface? In an attempt to understand such effects, we have examined a range of common anionic and cationic alkyl surfactants by TIR-SFVS and corresponding surface tension measurements.

Anionic surfactants account for the largest share of surfactant demand throughout the world. Of these, sodium dodecyl sulfate (SDS) is probably the most frequently studied, and it can be found in a range of commercial products. Cationic surfactants, specifically the ammonium salts, play an important role as sanitizing and antiseptic agents, germicides, fungicides, and components in many cosmetic formulations. Figure 2 shows the vibrational spectra of SDS and dodecylammonium chloride (DAC) at the  $\text{CCl}_4\text{-D}_2\text{O}$  interface, obtained by using the Nd:YAG-

pumped OPO system (15, 16, 28). The polarization combination  $S_{\text{sfg}}-S_{\text{vis}}-P_{\text{IR}}$  was used to probe SF active vibrational modes that have transition moments with components perpendicular to the plane of the surface.

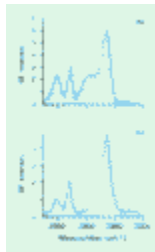


**Figure 2. Sum frequency vibrational spectra of (a) SDS and (b) DAC at the  $\text{CCl}_4\text{-D}_2\text{O}$  interface.**

Acquired with the polarization combination  $S_{\text{sfg}}-S_{\text{vis}}-P_{\text{IR}}$ . Bulk concentration of the surfactants was 5.0 mM. The solid lines represent a fit to the spectra using a combination of Gaussian and Lorentzian functions for each peak.

The spectra depicted correspond to bulk surfactant concentrations in which interfacial coverages reached a maximum (referred to here as a monolayer) as indicated by the interfacial tension measurements. Both surfactants are soluble in the aqueous phase and are at concentrations below the critical micelle concentration for each of the surfactants. Spectra of comparable S/N have been obtained for these surfactants at interfacial coverages down to 0.05 monolayer. Using the Ti:sapphire-pumped OPO system with the shorter pulse duration, our sensitivity improved by 2-3 orders of magnitude. The spectral features represent the C-H stretching modes of the methylene units in the backbone of the 12-carbon alkyl chain of the amphiphiles and the terminal methyl group. The methylene asymmetric stretch contributes to the strong intensity at  $2925\text{ cm}^{-1}$ . Peaks of moderate intensity are observed for the methylene symmetric and methyl symmetric stretches near  $2848\text{ cm}^{-1}$  and  $2872\text{ cm}^{-1}$ , respectively. Assignments of the spectral features have been confirmed by selective deuteration studies (29).

To ascertain the relative order of the alkyl chains in these molecules at this and other surface concentrations, the intensities of the methyl and methylene symmetric stretch

peaks in the SFG spectra are examined. The local symmetry of the CH<sub>2</sub> hydrocarbon backbone plays an important role in determining peak intensities of the CH<sub>2</sub> resonances. Under the electric dipole approximation for SFG, negligible contribution from methylene resonances should be observed for a system of well-ordered (all-trans) hydrocarbon chains (17).

As more gauche defects are introduced into the alkyl chain, the intensity of the methylene modes would be expected to increase as local symmetry constraints are relaxed. This phenomenon makes the methyl and methylene regions of the SF spectrum an especially sensitive indicator of alkyl chain conformation. Transition moments for the symmetric methyl and methylene modes for both gauche and trans conformations are illustrated in Figure 3. The presence of a significant methylene intensity (2850 cm<sup>-1</sup>) in both the SDS and DAC at this maximum interfacial coverage suggests a significant number of gauche defects in the hydrocarbon chain.

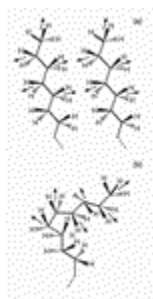


**Figure 3. Schematic representation of the net transition dipole moment for the symmetric methyl and methylene vibrational modes for (a) all-trans and (b) gauche conformations.**

The terminal methyl group, which possesses both IR and Raman active vibrational modes, is by nature in a noncentrosymmetric environment. Conformational information can be obtained from the relative intensity of the methyl peaks, which reflect the orientational average of the ensemble with respect to the surface normal. By judicious choice of the polarization of the incident optical beams and selection of appropriate output polarizations, the polarization dependence of the symmetric methyl stretch has been used to determine the average tilt angle of the hydrocarbon chain in these systems (17). For both

SDS and DAC, polarization studies show the terminal methyl group to point, on the average, along the surface normal (29). The orientation angle of specific bonds in the molecule of interest has been used frequently in previous studies (8, 11, 17). However, some limitations to these measurements are caused by the low signal levels for some polarization combinations used to determine bond orientation (6).

To illustrate how the conformational order of the alkyl chains varies with surface concentration, the ratio of the intensities of the symmetric methyl and symmetric methylene stretch modes has been used in many SFVS studies as an indicator of the relative order within the hydrocarbon chains (6, 11, 17, 28). A low methyl to methylene ratio reflects a relatively large number of gauche defects in the alkyl chain. In our studies of charged alkyl surfactants adsorbed at the  $\text{CCl}_4\text{-H}_2\text{O}$  interface, we consistently find that the greatest number of gauche defects are present at the lower interfacial concentrations. Increasing ordering of the alkyl chains is observed as the interfacial density of the surfactant increases.

Even at the highest interfacial coverages, however, all surfactants examined show significant alkyl chain disorder. This finding contradicts what is observed for many monolayers at solid-air and liquid-air interfaces, where the van der Waals interactions between the hydrophobic tails play an important role in monolayer stability. Furthermore, unlike many Langmuir layers at solid-air and liquid-air interfaces, we find the ordering of the chains to be indistinguishable for surfactants of consecutive even/odd chain lengths, providing additional evidence of the disruptive nature of the solvent on the van der Waals interactions between chains.

Interestingly, the cationic surfactants studied, including dodecyl trimethylammonium chloride, consistently show a higher degree of alkyl chain ordering than the anionic surfactants when compared at similar surface concentrations (29). Differences in their amphiphilic behavior are also manifested in their critical micelle concentrations, which are, for example, 8.2 mM for SDS and 14.0 mM for DAC. Because the surfactant molecular interactions in a micelle environment have many

similarities with surfactants at an oil-water interface, it is hoped that the liquid-liquid interfacial studies can be used to explain interactions in micelles and other structures in the bulk liquid.

### **Interfacial water structure and orientation**

Knowing the molecular properties of water at liquid interfaces and organized assemblies is a prerequisite for understanding various interfacial processes such as chemical reactivity, equilibria, proton transfer, and ion exchange. Recent research suggests that the most fundamental aspects of wetting phenomena are guided, to a large extent, by the structure and molecular properties of interfacial water. Structural features of interfacial water determine the nature of interaction forces that control flocculation and the preparation of thin films, dispersions, and emulsions. Water through solvation can have a significant effect on the rates of certain surfactant reactions and can participate as an interfacial reactant in spontaneous hydrolysis of numerous organic species such as acyl chlorides, acid anhydrides, and organic and inorganic esters.

We recently measured the first vibrational spectrum of water molecules at the interface between two bulk immiscible liquids (20). Our results demonstrate that the vibrational spectrum of water can be readily obtained at the oil-water interface using TIR-SFVS and that the presence of the  $\text{CCl}_4$  layer results in increased hydrogen bonding between water molecules at the interface relative to the air-water interface. These experiments used the Ti:sapphire-pumped OPA system so that the OH and OD vibrational stretches of  $\text{H}_2\text{O}$  and  $\text{D}_2\text{O}$  could be accessed (27).

Figure 4a shows a comparison of the vibrational spectrum of interfacial water at the air-water and  $\text{CCl}_4\text{-H}_2\text{O}$  interfaces (20). For the air-water interface, we found that two peaks are prominent in the O-H stretching region. The largest one at  $3200\text{ cm}^{-1}$  corresponds to the coupled OH symmetric stretch (SS) from symmetrically (S) bonded, tetrahedrally coordinated water molecules at the interface (OH-SS-S). At a quartz-ice interface, this "ice-like" peak dominates the SFV (19) spectrum. The second peak at  $3450\text{ cm}^{-1}$  (labeled OH-SS-A) is attributed to the

symmetric stretch of asymmetrically (A) bonded water molecules, arrangements of more "liquid-like" water that has incomplete tetrahedral coordination (lower degree of hydrogen bonding).



**Figure 4. SFV spectra of SDS.**

(a) H<sub>2</sub>O at the air-water interface (◼) and the CCl<sub>4</sub>-H<sub>2</sub>O interface (◯) and (b) H<sub>2</sub>O and SDS at the H<sub>2</sub>O-CCl<sub>4</sub> interface with increasing concentrations of SDS [(◯) 0.04 mM, (◼) 0.1 mM, and (▲) 2.06 mM] added to the bulk aqueous phase. The spectra were taken with the Ti:sapphire-pumped OPO with S<sub>sfg</sub>, S<sub>vis</sub> and P<sub>IR</sub> polarizations.

In contrast, the spectrum of water at the CCl<sub>4</sub>-H<sub>2</sub>O interface shows dominance of the icelike peak with an absence of any measurable signal from the higher energy mode, which suggests that the presence of the CCl<sub>4</sub> results in increased hydrogen bonding between interfacial molecules with the hydrophobic liquid phase placing a physical restriction on the water molecules. The small peak near 2950 cm<sup>-1</sup> is caused by minute traces of impurities in the system that concentrate over time at the interface. Trace amounts of impurity can be seen at the CCl<sub>4</sub>-H<sub>2</sub>O interface but not at the air-water interface because of the heightened sensitivity to interfacial structure and adsorbate concentration that the TIR geometry provides.

### **Adsorbed surfactants and the interfacial water orientation**

Another direction that our SFVS studies have taken is toward an understanding of how the structure and orientation of interfacial water are affected by the presence of charged surfactants (7, 30). The vibrational structure of both the interfacial water molecules and adsorbed surfactant are probed in these studies as

increasing amounts of surfactants are added to the aqueous phase. Figure 4b shows the SFV spectrum of SDS at the  $\text{CCl}_4\text{-H}_2\text{O}$  interface. In the C-H stretching region  $2600\text{-}3000\text{ cm}^{-1}$ , the response was similar to what we saw for SDS and DAC in that considerable gauche defects in the alkyl chains are apparent from the strong symmetric methylene contribution near  $2850\text{ cm}^{-1}$  (16, 29). The peaks' widths are different from those in Figure 2 because of the wider bandwidth of the Ti:sapphire system.

The most striking result from these studies occurs in the O-H stretch region corresponding to interfacial water. With increased surfactant concentration, a strong enhancement in the ice-like peak is observed relative to the surfactant-free interface. For similar SDS studies at the air-water interface, both the peaks shown in Figure 4a are enhanced as the surfactant adsorbs (7). Polarization studies show that these OH modes have a preferred orientation that is parallel to the surface normal.

We attribute this enhancement primarily to increased orientation of water molecules in the double-layer region, which is induced by the large electrostatic field created by the charged surfactant and counterion. Ionic strength studies support this conclusion. With increasing amounts of added NaCl, a decreased response from the O-H bands is observed. This effect can be understood in terms of a screening length that limits the number of interfacial water molecules that can interact with the electrostatic field as the ionic strength is increased (30). In the presence of the field, the depth sampling of the optical fields in the water surface region is on the order of the double-layer region, or the screening length. As this screening length is reduced with higher ionic strength, the number of aligned water molecules is reduced, as manifested in the reduced OH response.

Some general trends have emerged from these air-water and oil-water studies of interfacial water. For an uncharged surfactant, such as pentadecanoic acid in which the field in the double layer is minimal, the OH modes are barely detectable relative to the signal in the methyl stretch region, suggesting more random orientation of water molecules. For charged surfactants of different signs, the spectral features show that the water aligns in opposite directions depending on whether the surfactant

head group is cationic or anionic (7). This difference in alignment is manifested in an optical interference between C-H stretching modes and the OH symmetric stretch mode. This interference is constructive for the anionic surfactants and destructive for cationic surfactants, indicative of a change in phase of the OH response for the two different water orientations. For mixed surfactants, in which equal numbers of cationic and anionic surfactants are present, the OH enhancement does not occur, indicating a minimal field alignment of the water molecules caused by the reduced electrostatic field.

## **Phospholipids**

The phosphoglycerides, commonly referred to as phospholipids, are another class of surfactants that we have investigated. These biologically important surfactants, which comprise the major component of cell membranes, are generally composed of di-fatty acid, monophosphoric acid esters of glycerol combined with a polar head group that can be charged or neutral. Unlike the surfactants already described, phospholipids are generally insoluble in the bulk aqueous phase. Because they have good solubility in oil, these molecules have found extensive commercial application as nonaqueous emulsifiers, dispersants, and wetting agents in inks, foods, and cosmetics. Their unique molecular structure leads to the formation of interesting bilayer and vesicle structures in bulk aqueous solution.

One particularly interesting class of phospholipids is the phosphatidylcholines (PCs). The polar head group of these molecules consists of a negatively charged phosphate and a positively charged amine. At neutral pH, they exist as zwitterions with an ionizable negative charge on the phosphate and a positive charge on the ammonium ion. How these molecules might orient and order at an oil-water interface has been the focus of many theoretical studies over the past two decades, but experimental data to validate these predictions have been scarce.

The phosphocholines examined most extensively in our laboratory consist of saturated, symmetric, dialkyl species with alkyl chain lengths of 12 carbon atoms (dilauroyl-PC, DLPC), 14 carbon atoms (dimyristoyl-PC, DMPC), 16 carbon atoms (dipalmitoyl-PC, DPPC) and 18 carbon

atoms (distearoyl-PC, DSPC) (31). The aqueous phase is prepared by dissolving a given phosphocholine in a D<sub>2</sub>O-phosphate buffer at pH 7.0. The phospholipid suspension is sonicated above the lipid bilayer gel-liquid crystal-phase transition temperature, which produces unilamellar vesicles in the bulk aqueous phase (33). When these vesicles approach the CCl<sub>4</sub>-D<sub>2</sub>O interface, they are presumed to break apart to form monolayers at the interface by a mechanism that is currently unclear.

*... provides a better understanding of bilayer formation and molecular assembly of molecules important to biological processes.*

At room temperature, the SFV spectra and the surface pressure measurements show that at the CCl<sub>4</sub>-D<sub>2</sub>O interface the shortest chain phospholipid, DLPC, has the greatest surface activity and also displays the highest degree of conformational alkyl chain ordering throughout the concentration range studied. At its terminal interfacial pressure, the DLPC monolayer exhibits the closest packing with a molecular area of ~50 Å<sup>2</sup>/molecule. From the intensities of the C-H stretching modes in the SFV spectra, the dialkyl chains show a relatively high degree of ordering at this maximum coverage with fewer gauche defects than any of the simpler dodecyl surfactants. However, the strong methylene contribution at this interfacial concentration shows that the monolayers are not in an all-trans conformation. DMPC with its expanded monolayer (70 Å<sup>2</sup>/molecule) shows somewhat less surface activity and a correspondingly lower degree of conformational order than DLPC. The least surface-active PCs are DPPC and DSPC, which form the least ordered, and most expanded, monolayers.

Why phospholipids differing in only the length of their hydrocarbon chains exhibit such different behavior is intriguing. We believe that the answer lies in the physical properties of the different phosphocholine vesicles in aqueous solution. When fully hydrated, phospholipids spontaneously form vesicles, uni- or multilamellar bilayer structures (32). Two phases of vesicle lipid bilayers exist in the bulk phase: gel and liquid crystalline. Each

phospholipid has a characteristic phase-transition temperature  $T_c$  with the solid gel phase being the dominant bilayer structure at  $T < T_c$  and the liquid crystalline phase present for  $T > T_c$ . DLPC has a  $T_c$  of  $-1^\circ\text{C}$ . For the room-temperature experiments discussed above, the vesicle bilayers of DLPC exist in a disordered or liquid crystalline state, with relatively weak intermolecular forces between the hydrocarbon chains. The values of  $T_c$  for DPPC ( $41^\circ\text{C}$ ) and DSPC ( $55^\circ\text{C}$ ) indicate that the vesicle bilayers of these PCs are in the well-ordered gel phase.

Our spectral and isotherm data suggest that monolayer structure is correlated with  $T_c$ ; a low  $T_c$  (e.g.,  $-1^\circ\text{C}$  for DLPC) leads to high interfacial concentration and a high degree of order and vice versa. Temperature-dependent studies confirm this. When the temperature of the interface is raised above the  $T_c$  of the PC in solution, a much more tightly packed monolayer is formed with a corresponding higher degree of order as observed spectroscopically. Also at this higher temperature, a correspondingly higher interfacial pressure is measured that is comparable to the terminal pressure of DLPC at room temperature.

Consistent results are also found for DMPC and DPPC, which leads us to conclude that the thermodynamics of monomer dissociation from the vesicles controls the interfacial concentration and hence the structure of phospholipids adsorbed to the interface. Interestingly, when the four phospholipid monolayers have equivalent interfacial concentrations, the longer chain phospholipids, even when tightly packed, still sustain a greater number of gauche defects, leading to a greater conformational disorder within the monolayer. This is the reverse of the trend that we observe for these PCs at the air-water interface.

Additional studies of deuterated PCs have been conducted to isolate the response from C-H modes in the head group region of the phospholipids. The data allow us to learn about the head group orientation and environment of these phospholipids at the  $\text{CCl}_4\text{-H}_2\text{O}$  interface. Studies of the structure and orientation of the water molecules at the interface in the presence of phospholipids have also been conducted. Less enhancement in the orientation of water

in the double layer is observed relative to the alkyl surfactants, as might be expected because of the zwitterionic nature of the phospholipids.

### **Tip of the iceberg**

These first vibrational spectroscopic studies of interfaces between two immiscible liquids show that valuable new insight is possible using TIR-SFVS. The studies completed thus far are only the tip of the iceberg of what can be done in studying molecular processes at liquid-liquid interfaces. A host of surfactants could readily be studied, including other ionic surfactants, nonionic surfactants, and polymers. With extended wavelength tunability to access other vibrational modes of the surfactants in the head group region, the potential exists to obtain a better understanding of solvation of the head group and its interfacial environment.

By simultaneously measuring the spectrum of interfacial solvent molecules in the presence and absence of surfactants, a better picture should emerge of how the molecular structure of interfacial molecules affects the measured thermodynamic behavior of liquid-liquid interfaces. For biologically relevant molecules, studies in this area provide a means of obtaining a better understanding of bilayer formation and molecular assembly of molecules important to a host of biologically important processes.

The projects described in this paper were funded by the National Science Foundation (CHE-9416856), the Office of Naval Research, and the Petroleum Research Fund of the American Chemical Society. I also thank D. E. Gragson and R. A. Walker for assistance in preparing this manuscript.

### **References**

- (1) Lu, J. R.; Lee, E. M.; Thomas, R. K.; Penfold, J.; Flitsch, S. L. *Langmuir* **1993**, *9*, 1353.
- (2) Shih, M. C.; Bohanon, T. M.; Mikrut, J. M.; Zschack, P.; Dutta, P. *Phys. Rev. A* **1992**, *45*, 5374.
- (3) Buontempo, J. T.; Rice, S. A. *J. Chem. Phys.* **1993**, *98*, 5835.

- (4) Fischer, B.; Tsao, M-W.; Ruiz-Garcia, J.; Fischer, T. M.; Schwartz, D. K.; Knobler, C. M. *J. Phys. Chem.* **1994**, *98*, 7430.
- (5) Qiu, X.; Ruiz-Garcia, J.; Stine, K. J.; Knobler, C. M.; Selinger, J. V. *Phys. Rev. Lett.* **1991**, *67*, 703.
- (6) Bell, G. R.; Bain, C. D.; Ward, R. N. *J. Chem. Soc. Faraday Trans.* **1996**, *92*, 515.
- (7) Gragson, D. E.; McCarty, B. M.; Richmond, G. L. *J. Phys. Chem.* **1996**, *100*, 14272.
- (8) Shen, Y. R. *Nature* **1989**, *337*, 519.
- (9) Richmond, G. L.; Robinson, J. M.; Shannon, V. L. *Prog. Surf. Sci.* **1988**, *28*, 1.
- (10) Corn, R. M.; Higgins, D. A. *Chem. Rev.* **1994**, *94*, 107.
- (11) Eiseenthal, K. B. *Chem. Rev.* **1996**, *96*, 1343.
- (12) Wirth, M. J.; Burbage, J. D. *J. Phys. Chem.* **1992**, *96*, 9022.
- (13) Conboy, J. C.; Richmond, G. L. *J. Phys. Chem.* **1997**, *101*, 983.
- (14) Conboy, J. C.; Daschbach, J. L.; Richmond, G. L. *J. Phys. Chem.* **1994**, *98*, 9688.
- (15) Messmer, M.; Conboy, J. C.; Richmond, G. L. *J. Am. Chem. Soc.* **1995**, *117*, 8040.
- (16) Conboy, J. C.; Messmer, M. C.; Richmond, G. L. *J. Phys. Chem.* **1996**, *100*, 7617.
- (17) Hunt, J. H.; Guyot-Sionnest, P.; Shen, Y. R. *Chem. Phys. Lett.* **1987**, *133*, 189.
- (18) Wolfrum, K.; Laubereau, A. *Chem. Phys. Lett.* **1994**, *228*, 83.
- (19) Du, Q.; Freysz, E.; Shen, Y. R. *Science* **1994**, *264*, 826.

- (20) Gragson, D. E.; Richmond, G. L. *Langmuir*, **1997**, *13*, in press.
- (21) Stanners, C. D.; Du, Q.; Chin, R. P.; Cremer, P.; Somorjai, G. A.; Shen, Y. R. *Chem. Phys. Lett.* **1995**, *232*, 407.
- (22) Zhang, D.; Gutow, J. H.; Eienthal, K. B.; Heinz, T. *F. J. Chem. Phys.* **1994**, *98*, 5099.
- (23) Harris, A. L.; Rothberg, L.; Dhar, L.; Levinos, N. J.; Dubois, L. H. *J. Chem Phys.* **1991**, *94*, 2438.
- (24) Guyot-Sionnest, P.; Tadjeddine, A. *Langmuir* **1990**, *5*, 172.
- (25) Guyot-Sionnest, P.; Superfine, R.; Hunt, J. H.; Shen, Y. R. *Chem. Phys. Lett.* **1988**, *144*, 1.
- (26) Epperlein, D.; Dick, B.; Marowsky, G.; Reider, G. A. *Appl. Phys. B* **1987**, *44*, 5.
- (27) Gragson, D. E.; McCarty, B. M.; Richmond, G. L.; Alavi, D. S. *J. Opt. Soc. B* **1996**, *13*, 1492.
- (28) Conboy, J. C.; Messmer, M. C.; Walker, R.; Richmond, G. L. *Prog. Coll. Polym. Sci.* **1997**, *103*, 10.
- (29) Conboy, J. C.; Messmer, M. C.; Richmond, G. L. *J. Phys. Chem.*, **1997**, *101*, in press.
- (30) Gragson, D. E.; McCarty, B. M.; Richmond, G. L. *J. Am. Chem. Soc.* **1997**, *119*, 6144.
- (31) Walker, R. A.; Conboy, J. C.; Richmond, G. L. *Langmuir* **1997**, *13*, 3070.
- (32) Szoka, F.; Papahadjopoulos, D. *Ann. Rev. Biophys. Bioeng.* **1980**, *9*, 467.

*Geraldine Richmond is professor of chemistry at the University of Oregon. Address correspondence about this article to Richmond at Dept. of Chemistry, University of Oregon, Eugene, OR 97403.*

anchama 69> 17 4170-sep01.report2